Available online at www.sciencedirect.com
SCIENCE DIRECT®
Journal of Photochemistry and Photobiology A: Chemistry 173 (2005) 185–194
Journal of Photochemistry and Photobiology A:Chemistry
www.elsevier.com/locate/jphotochem

Photochemical synthesis and optical properties of binary and ternary metal–semiconductor composites based on zinc oxide nanoparticles

A.L. Stroyuk *, V.V. Shvalagin, S.Ya. Kuchmii

Pysarzhevsky Institute of Physical Chemistry, National Academy of Sciences of Ukraine, 31 Nauky Av., 03028 Kyiv, Ukraine

Received 15 October 2004; received in revised form 6 February 2005; accepted 9 February 2005
Available online 7 March 2005

Abstract

Photochemical properties of zinc oxide nanoparticles and their photocatalytic activity in the processes of the reduction of Cu^{2+} and Pb^{2+} ions as well as mixtures of Cu^{2+}–Ag^{+} and Cd^{2+}–Ag^{+} ions have been investigated. Optical properties of ZnO/Cu, ZnO/Pb, ZnO/Ag/Cu, ZnO/Ag/Cd and ZnO/Ag/Zn nanocomposites have been examined.

It has been found that a decrease in the size of ZnO nanoparticles from 6.0 nm to 4.4 nm results in the strengthening of quantum confinement of photogenerated charge carriers, growth of the band gap and the potentials of the conduction band and the valence band of the semiconductor. It has been found that ZnO nanoparticles smaller than $2R = 6.0$ nm photocorrode with the formation of metallic zinc when the colloidal solution is irradiated with the mild UV light. An increase in the potential of the conduction band electrons and the ability of ZnO nanoparticles to accumulate excessive negative charge have been supposed to be the principle reasons of advanced photochemical activity of ZnO nanoparticles with $2R < 6.0$ nm.

Mie theory has been applied to analyze the parameters of surface plasmon resonance bands of metallic copper in ZnO/Cu nanocomposites as well as to estimate an average size of Cu^{0} nanoparticles formed on the surface of the semiconductor.

It has been found that Cu(II) photoreduction rate increases substantially when Ag^{+} ions are present in the irradiated systems. Photocatalytic reactions in these systems result in the formation of ternary bimetallic ZnO/Ag/Cu nanocomposites.

It has been shown that Cd(II) ions, which are stable towards photoreduction on the surface of ZnO nanoparticles, can be co-reduced with Ag^{+} cations giving ternary ZnO/Ag/Cd nanocomposites with peculiar optical properties. Correlations between the conditions of co-reduction of metal cations and the parameters of partially disturbed silver plasmon bands in the optical spectra of colloidal ZnO/Ag/Cd and ZnO/Ag/Zn have been established.

Keywords: Photocatalysis; Photocorrosion; Photochemical synthesis; ZnO nanoparticles; Quantum confinement effects; Copper nanoparticles; Metal–semiconductor nanocomposites

1. Introduction

Photochemical reduction of the cations of some metals (for example, Ag, Au, Cu, Pt, Pd, Cd, etc.) induced by semiconductor nanoparticles (TiO_2, ZnO, SnO_2, CdS, ZnS, etc.) are of great interest not only as model processes for the investigation of photocatalytic properties of ultradispersed semiconductors, but also as one of the methods of the preparation of nanostructured metal–semiconductor composites [1–11]. An advantage of this method lies in the opportunity to control the composition of metal–semiconductor nanostructures through variations in the conditions of photochemical reaction [1,2,5,9,11–13]. This method can be successfully applied for the synthesis of multicomponent composites consisting of semiconductor nanocrystals and several metals in the form of alloy or "core–shell" structure [14].

Metal–semiconductor nanostructures manifesting properties of the semiconductor and the metal find wide application in photocatalysis due to the ability of metallic component to accumulate electrons generated at the absorption of light by the semiconductor component. Accumulation of

* Corresponding author. Tel.: +380 44 265 0270; fax: +380 44 265 6295.
E-mail address: stroyuk@inphyschem-nas.kiev.ua (A.L. Stroyuk).

1010-6030/$ – see front matter © 2005 Elsevier B.V. All rights reserved.
doi:10.1016/j.jphotochem.2005.02.002

electrons within the metal "pool" of the nanocomposite improves primary charge separation and boosts photocatalytic [1–7,10–12,15,16] and photoelectrocatalytic [8,17] activity of the semiconductor.

In case of the semiconductor nanoparticles with quantum confinement effects, photochemical reactions can sometimes be performed, having no analogues in the world of bulk (micrometer) semiconductor crystals. The effects of quantum confinement may substantially affect both optical and photochemical properties of ultradispersed semiconductors [3,12]. These effects originate from the changes in energetic characteristics of charge carriers photogenerated in semiconductor crystals as small as exciton delocalization domain (typical range of this domain is 1–10 nm) [3,18]. Growth of absolute potentials of conduction band electrons and valence band holes, at a decrease in the size of nanoparticles, may lead to substantial increase in photochemical and photocatalytic activity of ultradispersed semiconductor. Cases, when size-dependent alterations of energetic characteristics of charge carriers give rise to redox processes, which are thermodynamically forbidden for bulk crystals of the semiconductor, are of particular interest. The vivid example of the latter phenomenon is the process of cathodic photocorrosion of zinc oxide nanoparticles (the bulk crystals of this semiconductor are stable towards the reductive photocorrosion [19]) resulting in the formation of composite ZnO/Zn nanoparticles. We also discuss some peculiarities of the photochemical synthesis of binary (ZnO/Cu and ZnO/Pb) and ternary (ZnO/Ag/Cu, ZnO/Ag/Cd and ZnO/Ag/Zn) nanostructures, evolution of their absorption spectra in the course of the synthesis and the effect of photoreduction conditions on the optical properties of the nanocomposites.

2. Experimental

ZnO nanoparticles in 2-propanol have been synthesized via the basic hydrolysis of zinc acetate (reagent grade) by sodium hydroxide (pure) at 0 °C [20–23]. In typical procedure, dry powdered $Zn(CH_3COO)_2$ (0.0915 g, 0.5 mmol) is dissolved at continuous refluxing in 60 ml of anhydrous twice-distilled 2-propanol at 50–60 °C. Resulting solution is diluted to 230 ml by 2-propanol and cooled to 0 °C again. Powdered NaOH (0.032 g, 0.8 mmol) is dissolved in 20 ml of anhydrous 2-propanol at 50–60 °C and then cooled to 0 °C. Solutions of sodium hydroxide and zinc acetate are slowly mixed at intense refluxing at 0 °C. After the synthesis, colloidal ZnO solution is heated for 2 h at 55–60 °C. Final colloidal ZnO solution has an absorption band with steep long-wave edge at 365–370 nm and contains spherical ZnO nanocrystals with the average diameter 5 ± 0.5 nm [20,21].

Colloidal solutions of zinc oxide in ethanol have been prepared in the same way from zinc acetate, sodium hydroxide in anhydrous ethyl alcohol. Solutions of Ag(I), Cu(II) and Pb(II) have been prepared from reagent grade $AgNO_3$, $CuCl_2$ and $Pb(CH_3COO)_2$.

Composite ZnO/Ag nanoparticles have been synthesized in ethanol and 2-propanol similar to [13] via photocatalytic reduction of $AgNO_3$ on the surface of ZnO nanoparticles. Irradiation of the solution containing $[ZnO] = 1 \times 10^{-3}$ M and $[AgNO_3] = 7.5 \times 10^{-5}$ M to 1×10^{-4} M up to complete conversion of Ag^+ ions results in the formation of ZnO/Ag nanocomposite with the average size of Ag^0 nanoparticles 1.8–2.0 nm [13].

Solutions have been irradiated in glass parallel-sided 1.0 cm cuvettes with the filtered light of 1000 W mercury high-pressure lamp. Glass 5.0 cm cuvette filled with water has been placed between the light source and the work cuvette to avoid heating of the latter. Light intensity was adjusted by calibrated metal semi-transparent filters and measured by ferrioxalate actinometry.

Optical spectra were registered using Specord M-40 double-beam spectrophotometer (spectral range 185–900 nm, resolution 0.1 nm, precision of absorbance measurements 0.005).

3. Results and disscussion

3.1. Synthesis, optical and photochemical properties of ZnO colloids; formation of binary ZnO/Zn nanocomposites

Basic hydrolysis of zinc acetate by sodium hydroxide in 2-propanol is well studied, reproducible and comparatively simple method of the preparation of colloidal ZnO nanoparticles [20–23]. We have found that analogous procedure may also be carried out in ethyl alcohol. The latter method has two advantages. First one lies in a possibility to synthesize more concentrated (up to 2×10^{-2} M) zinc oxide colloids as compared with 2-propanolic solutions, where ZnO nanoparticles become unstable already at $[ZnO] > 2 \times 10^{-3}$ M. The second advantage is simple control of the size of ZnO nanoparticles through variations in reagents' concentrations. Fig. 1 shows absorption spectra of ethanolic ZnO colloids of two different concentrations. At a decrease of zinc oxide concentration

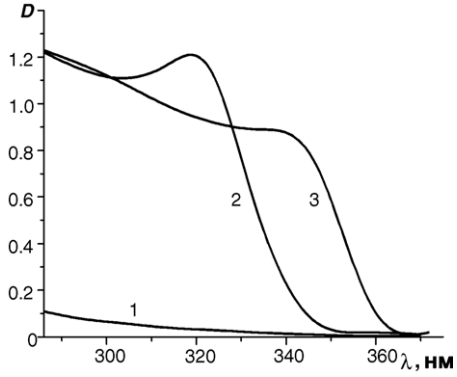

Fig. 1. Absorption spectra of colloidal ZnO solutions in ethanol after the mixing of the reagents (1), after 2 h ageing at 55–60 °C; $[ZnO] = 1 \times 10^{-3}$ M in (2) and 2×10^{-2} M in (3).

from 2×10^{-2} M to 1×10^{-3} M, long-wave edge of the absorption band of a colloid shifts from 365 nm to 345 nm. This shift is caused by strengthening of the quantum confinement of charge carriers at a decrease in the size of ZnO nanoparticles [20–23]. From the position of long-wave edge of the fundamental absorption band, an important characteristic of the semiconductor – the band gap, E_g – may be easily calculated. Band gaps of ZnO nanoparticles have been calculated from the values of light quantum energy corresponding to the wavelength at the cross point between the axis of abscissae and a tangent to long-wave edge of the absorption band in electronic spectra of ZnO colloids. The hypsochromic shift of the position of the band edge from 365 nm to 354 nm corresponds to the increase of E_g value of ZnO nanoparticles from 3.42 eV to 3.63 eV. Average diameters of ZnO nanoparticles ($2R$) may then be estimated from the E_g values using the approximation of effective masses and Equation (I) [20,24]:

$$\Delta E_g = \frac{\hbar^2\pi^2}{2R^2}\left(\frac{1}{m_e^* m_0} + \frac{1}{m_h^* m_0}\right) - \frac{1.8e^2}{4\pi\varepsilon\varepsilon_0 R} - \frac{0.124e^4}{\hbar^2(4\pi\varepsilon\varepsilon_0)^2}\left(\frac{1}{m_e^* m_0} + \frac{1}{m_h^* m_0}\right)^{-1} \quad \text{(I)}$$

where ΔE_g is an odds between E_g values of colloidal and bulk zinc oxide (for bulk ZnO $E_g^{bulk} = 3.2$ eV [20,21,24,25]), R the radius of ZnO nanoparticles, $\hbar$ the reduced Planck's constant, m_e^*, m_h^* the effective masses of conduction band electrons and valence band holes, correspondingly (for ZnO $m_e^* = 0.26$, $m_h^* = 0.59$ [24]), m_0, e the rest mass and the charge of electron and ε, ε_0 are the dielectric permeabilities of zinc oxide ($\varepsilon = 8.5$ [24]) and dispersive medium, correspondingly.

Estimations based on Equation (I) have shown that the increase of E_g value of Zn nanoparticles from 3.42 eV to 3.63 eV corresponds to the decrease of the average size of nanoparticles from $2R = 6.0$ nm to 4.4 nm. It should be noted that steep fall of the absorption band near the edge indicates that colloidal ZnO solutions are highly monodisperse [20,21,24].

The irradiation of a deaerated ZnO solution with $E_g = 3.63$ eV results in a hypsochromic shift of the long-wave edge of the absorption band. Magnitude of this shift (ΔE_{hv}, eV) grows at an increase of the exposure (Fig. 2). This shift originates from an increase in the optical band gap of the semiconductor in the result of an accumulation of excessive of electrons in surface traps of nanocrystals (dynamic Burstein–Moss effect) [1,20,21]:

$$ZnO + hv \rightarrow ZnO(e_{CB}^- + h_{VB}^+) \quad (1)$$

$$ZnO(h_{VB}^+) + CH_3CH_2OH \rightarrow CH_3CH^{\bullet}OH + H^+ \quad (2)$$

$$ZnO(e_{CB}^-) \rightarrow ZnO(e_{tr}^-) \quad (3)$$

where e_{tr}^- is an electron trapped in a surface defect, e_{CB}^- and h_{VB}^+ are the conduction band electrons and the valence band holes.

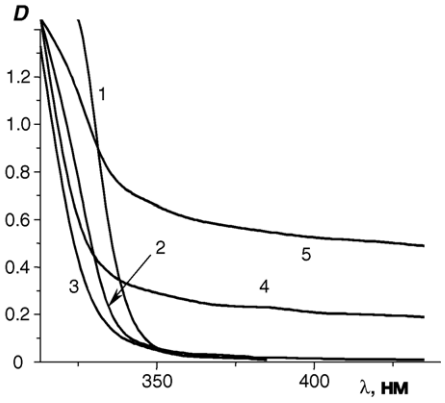

Fig. 2. Absorption spectrum of a colloidal ZnO solution in ethyl alcohol before the irradiation (1) and after the exposure for 10 min (2), 20 min (3), 40 min (4) and 60 min (5); light intensity $I = 3.5 \times 10^{-6}$ einstein min^{-1}, $\lambda_{irr} = 310$–370 nm; [ZnO] = 1×10^{-3} M.

Oxyethyl radicals generated in reaction (2) decay predominantly via electron injection into zinc oxide nanoparticles [26]:

$$CH_3CH^{\bullet}OH + ZnO \rightarrow CH_3CHO + H^+ + ZnO(e_{tr}^-) \quad (4)$$

Admission of the air into the cuvette results in fast recovery of initial position of band edge due to fast reaction of excessive electrons with oxygen:

$$e_{tr}^- + O_2 \rightarrow O_2^{\bullet -} \quad (5)$$

At $\Delta E_{hv} = 0.15$–0.16 eV, the band edge position of ZnO nanoparticles remains constant. Further irradiation of the solution results in the growth of the absorbance within the whole measured spectral domain (Fig. 2). At that the colloidal solution becomes grey–brown. The solution retains its colour at prolonged storage in the dark in the absence of the air. Upon the admission of the air to the cuvette, the solution becomes colourless again, while the band edge recovers its initial position. Passivity of the coloured photoproduct towards alcohols coupled with its high reactivity towards molecular oxygen indicates that the photoproduct has reductive nature. Taking into account that ZnO nanoparticles can catalyze photoreduction of a number of metals (Ag, Cu, Au, Pt, etc. [1,13]), we have attributed the observed reversible changes of the absorbance spectra of ZnO colloid to the formation of metallic zinc on the surface of zinc oxide nanoparticles. Since Zn^0 does not have characteristic features (such as plasmon maxima, bends, etc.) in the spectral region between 300 nm and 700 nm, we have used the value of the optical density of the solution at arbitrarily chosen wavelength ($\lambda = 375$–380 nm), after 60 min exposure (ΔD_{60}) as an equivalent of the rate of photochemical reaction.

Colloidal ZnO solutions contain 20% excess of $Zn(CH_3COO)_2$ over molar ZnO concentration, so one may suppose that Zn^0 appears as a result of the photoreduction of zinc acetate or its partially hydrolized hydroxocomplexes. It

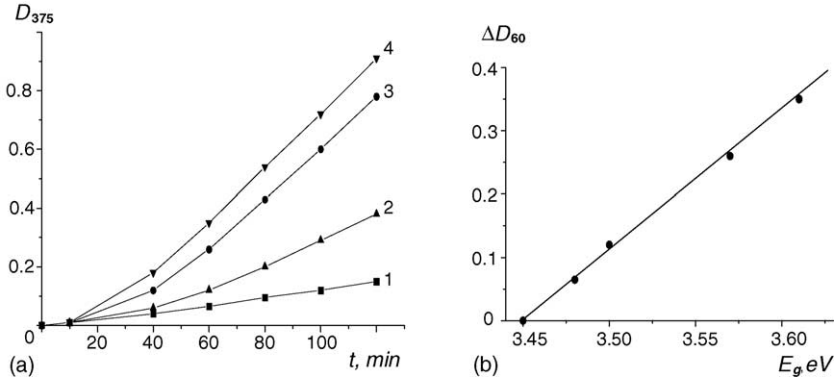

Fig. 3. (a) Growth of the optical density of deaerated colloidal ZnO solutions at 375 nm (D_{375}) under the irradiation into 310–370 nm window. Average size of ZnO particles is 5.5 nm (1), 5.2 nm (2), 4.8 nm (3) and 4.4 nm (4); optical path $l = 1.0$ cm; $[ZnO] = 1 \times 10^{-3}$ M. (b) A correlation between the rate of ZnO photocorrosion and the band gap of the semiconductor nanoparticles.

has been found, however, that the rate of photoproduct accumulation neither depends on the concentration of zinc acetate (which has been varied from 1×10^{-3} M to 5×10^{-3} M) nor lowers at an addition of NaOH (2×10^{-3} M to 5×10^{-3} M) able to bind zinc(II) ions.

Alternative interpretation of experimental results consists in the assumption that irradiation-induced changes of absorption spectra of ZnO colloids result from the cathodic photocorrosion of zinc oxide:

$$ZnO + 2e_{tr}^- + H_2O \rightarrow Zn^0 + 2OH^- \qquad (6)$$

It has been found that the rate of ZnO photocorrosion lowers substantially at an increase in the size of nanoparticles (Fig. 3a). In case of the biggest of studied ZnO nanoparticles ($2R = 6.0$ nm), we have not observed Zn^0 formation at all. It should be noted that the magnitude of the shift ΔE (calculated from a hypsochromic shift of the optical edge of the fundamental absorption band) necessary to induce Zn^{2+} photoreduction is almost the same for ZnO nanoparticles of different size and is equal to 0.15 eV, while the rate of the photoreaction increases linearly with an increase in E_g value of ZnO nanoparticles, i.e. at a decrease in their average diameter.

It is evident that ZnO photocorrosion described by the brutto Equation (6) does not require the participation of any reactants other than ZnO nanoparticles and solvent molecules. So, it may be concluded that: (i) the photocorrosion is not limited by the diffusion of any reactant to the surface of ZnO nanoparticles and (ii) an increase in the rate of the photocorrosion at a decrease in the size of ZnO nanoparticles results from a change of the properties of photogenerated charge carriers.

The potentials of the conduction band (E_{CB}) and the valence band (E_{VB}) of ZnO nanoparticles may be estimated with the use of expressions (II) [27].

$$E_{CB} = E_{CB}^{bulk} - \Delta E_{CB}; \qquad E_{VB} = E_{VB}^{bulk} + \Delta E_{VB}, \qquad (II)$$

where

$$\Delta E_{CB} = \frac{\hbar^2}{8m_e^* R^2}; \qquad \Delta E_{VB} = \frac{\hbar^2}{8m_h^* R^2}$$

E_{CB}^{bulk} and E_{VB}^{bulk} are the potentials of bulk zinc oxide ($E_{CB}^{bulk} = -0.42$ V versus normal hydrogen electrode (NHE) at pH 7, $E_{VB}^{bulk} = 2.78$ V versus NHE at pH 7 [27]) and $\hbar$ is reduced Planck's constant.

The potentials of the conduction and valence bands of ZnO nanoparticles of different size estimated with the use of Equation (II) are shown in Table 1. Quantum confinement effect, becoming more expressed at the decrease in the size of ZnO nanocrystals from $2R = 6.0$ nm to 4.4 nm, results in the growth of ZnO conduction band potential from −0.58 V to −0.72 V versus NHE. Zinc oxide photoreduction begins only after an accumulation of certain excessive negative charge by ZnO nanoparticles, i.e. under cathodic polarization. Accumulation of excessive electrons by ZnO nanoparticles results in the degeneration of the semiconductor and a shift of its Fermi level (E_F) from the band gap into the conduction band [1,13]. Magnitude of $E_F - E_{CB}$ is proportional to the density of ex-

Table 1
Energetic characteristics of ZnO nanoparticles of different size

E_g (eV)	E_{CB} (V) (vs. NHE)	E_{VB} (V) (NHE)	$2R$ (nm)	E^* (V) (NHE)	$E^* - E_{corr}$ (V)
3.43	−0.58	2.85	6.0	−0.78	0.02
3.48	−0.61	2.86	5.5	−0.81	−0.01
3.50	−0.63	2.87	5.3	−0.83	−0.03
3.57	−0.68	2.89	4.8	−0.88	−0.08
3.63	−0.72	2.91	4.4	−0.92	−0.12

cessive electrons and may be calculated from the optical shift ΔE with the use of expression (III) [13,28].

$$\Delta E = \left(1 + \frac{m_e^*}{m_h^*}\right)(E_F - E_{CB} - 4kT) \quad \text{(III)}$$

where k is Boltzmann constant.

The shift of the edge of fundamental absorption band $\Delta E_{hv} = 0.15$ eV corresponds to $E_F - E_{CB} = 0.20$ eV ($4kT = 0.1$ eV at 297 K). Adding this value to the potentials of 6.0–4.4 nm ZnO nanoparticles (Table 1), we may deduce that the conduction band potential of cathodically polarized ZnO nanoparticles (E^*) varies from −0.78 V ($2R = 6.0$ nm) to −0.92 V ($2R = 4.4$ nm).

According to [25], reductive decomposition of 5–6 nm ZnO nanoparticles may be expected to start at the potentials more negative than $E_{corr} = -0.8$ V (versus NHE). Comparison of E_{corr} with calculated E^* values for ZnO nanoparticles of different size (Table 1) shows that the photocorrosion is thermodynamically unprobable for 6.0 nm ZnO nanoparticles, but may occur in case of smaller nanocrystals. Experimental results confirm this conclusion. It should be also noted that linear growth of the rate of zinc oxide photocorrosion at a decrease in the size of the nanoparticles (Fig. 3b) agrees well with Tafel equation applied for the case of small overvoltages [29], which predicts linear correlation between the rate of electrochemical reaction and the magnitude of electrode overvoltage, i.e. the value of $E^* - E_{corr}$.

3.2. ZnO–Cu(II) system

It has been established that the irradiation of deaerated ZnO sols in ethanol or 2-propanol in the presence of $CuCl_2$ results in the rise of new intense band in the absorption spectrum of solutions. This band falls monotonously towards the long-wave side of the spectrum and has a maximum at 600–610 nm (Fig. 4a and b). According to [30–36], such absorption bands belong to ultradispersed Cu^0 particles and arise from collective resonant oscillation of electron gas within the surface layer of metal nanoparticles in the electromagnetic field of light wave (surface plasmon resonance (SPR) bands). Hypsochromic shift of ZnO absorption band is not observed in the presence of Cu(II), indicating that the reactions of photogenerated ZnO conduction band electrons with metal ions are fast. Hence, we have concluded that the irradiation of ZnO colloids in the presence of $CuCl_2$ results in the formation of Cu^0 nanoparticles on the surface of the semiconductor:

$$Cu^{2+} + 2e_{tr}^-(ZnO) \rightarrow ZnO/Cu^0 \quad (7)$$

Cu(II) can be photoreduced in two ways: (i) via one-electron mechanism with the formation of Cu(I) and its subsequent disproportionation to Cu(0) and Cu(II) and (ii) via two-electron mechanism, the last being especially probable in alcohols, which are not able to stabilize Cu(I) [29,37]. In both cases, Cu(II) photoreduction by the electrons photogenerated in the conduction band of 5.0 nm ZnO nanoparticles ($E_{CB} = -0.63$ V versus NHE, Table 1) is thermodynamically allowed since $E^0(Cu^{2+}/Cu^+) = +0.153$ V, $E^0(Cu^+/Cu^0) = +0.52$ V and $E^0(Cu^{2+}/Cu^0) = +0.337$ V versus NHE [29].

Copper photoreduction is not observed in the presence of oxygen able to react with e_{tr}^- (reaction (5)). Assuming that Cu(II) photoreduction is equiprobable on the surface of each ZnO nanoparticle (i.e. the number of forming metal particles is equal to the number of ZnO nanoparticles), we may use Mie approximation [30,36] to estimate an average volume of the metal per particle, V, as well as the radius of nanoparticles, R, from the position of the maximum of copper SPR band, λ_{max}, and the width of the plasmon band measured on the half of its height in the maximum, w (Fig. 4b):

$$R = \left(\frac{3V}{4\pi}\right)^{1/3} = \left[\frac{D_{max}(\varepsilon_0 + 2n_0^2)[(\lambda_{max}^2 - \lambda^2)^2 + \lambda^2\varpi^2]}{24\pi^2 N n_0^3 \lambda^2 \varpi}\right]^{1/3} \quad \text{(IV)}$$

where D_{max} is the optical density of plasmon absorption band in the maximum, ε_0 the dielectric permeability of the metal, n_0 the refraction index of dispersive medium, $\lambda = \lambda_{max} - \frac{1}{2}w$

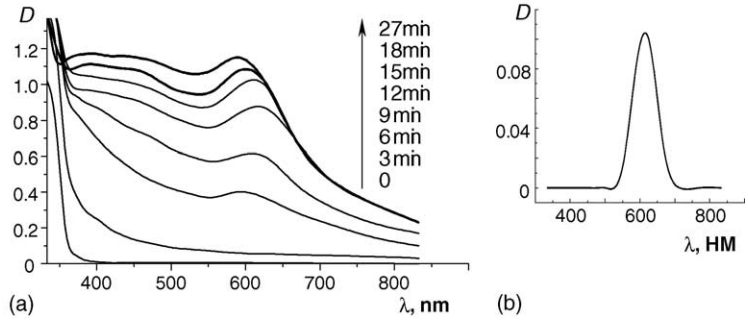

Fig. 4. (a) Absorption spectra of a deaerated colloidal ZnO solution containing $CuCl_2$ before the irradiation and after 3–27 min exposures. (b) Plasmon absorption band of copper nanoparticles extracted from the absorption spectrum of ZnO/Cu nanocomposite after 12 min illumination; $[ZnO] = 2 \times 10^{-3}$ M; $[CuCl_2] = 5 \times 10^{-4}$ M; light intensity $I = 3.3 \times 10^{-6}$ einstein min^{-1}.

and N is the numeric concentration of ZnO nanoparticles in a solution.

Estimations based on Equation (IV) have shown that SPR band presented in Fig. 4b corresponds to Cu^0 nanoparticles with $2R = 1.6$ nm composed in the average of 200–210 copper atoms.

Fig. 4a shows that after a certain period of the irradiation, the growth of the intensity of copper plasmon band gradually slows down and stops due to complete consumption of $CuCl_2$. It was found that maximal intensity of copper plasmon band, i.e. the intensity of plasmon band achieved at complete reduction of Cu(II) cations, grows linearly with an increase in the initial concentration of copper salt, the extinction coefficient in the maximum of Cu^0 plasmon band $\varepsilon_{Cu} = 2400–2600\ M^{-1}\ cm^{-1}$. Quantum yields of the photoreduction of Cu(II) on the surface of ZnO nanocrystals, γ_{Cu}, calculated with the use of Equation (V), have been found to be 0.018–0.020.

$$\gamma_{Cu} = \varepsilon_{Cu} \cdot D_{max} \cdot v_{cuv} \cdot (I \cdot t \cdot 1000)^{-1} \quad \text{(V)}$$

where v_{cuv} is the volume of a solution in the cuvette, I the light intensity (in einstein min^{-1} = quanta mol min^{-1}) and t is the exposure (in min).

Fig. 4a shows that a hypsochromic shifts both of the maximum of copper SPR band and of the position of the edge of ZnO absorption band are observed on final stage of the photoreaction. According to [30,36] the position of the maximum of SPR band is determined mainly by the nature of a medium, dielectric parameters of a metal and the density of electron gas N_e:

$$\lambda_{max}^2 = \frac{(2\pi c)^2 m_e(\varepsilon_0 + 2n_0^2)}{4\pi e^2 N_e} \quad \text{(VI)}$$

where c is the light velocity in vacuum.

Analysis of the expression (VI) shows that an increase in the density of free electrons in the volume of metallic nanoparticle should result in a hypsochromic shift of the maximum of SPR absorption band. A shift of the edge of ZnO absorption band is also induced by an accumulation of excessive electron in surface traps of the semiconductor. Hence, after complete consumption of $CuCl_2$ in a solution, the irradiation of ZnO/Cu system results in the accumulation of electrons on both components of the nanocomposite. It should be noted that this is possible only in case of strong electronic interaction between the semiconductor and the metal [1,2,13].

Kinetic curves of Cu^0 accumulation have the shape of the letter S (Fig. 5), typical for autocatalytic reactions. Autocatalysis in the system under examination may arise from the ability of growing copper nanoparticles to accumulate electrons (i.e. act as nanometer electrodes–collectors) and to adsorb Cu(II) cations facilitating in that way their photoreduction.

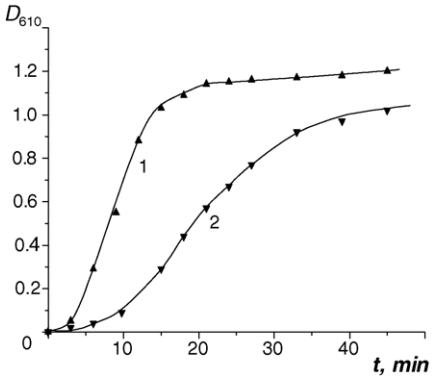

Fig. 5. Kinetic curves of Cu^0 accumulation at the irradiation of deaerated ethanolic (1) and 2-propanolic (2) colloidal ZnO solutions in the presence of $CuCl_2$; $[ZnO] = 2 \times 10^{-3}$ M; $[CuCl_2] = 5 \times 10^{-4}$ M; light intensity $I = 3.3 \times 10^{-6}$ einstein min^{-1}.

3.3. ZnO–Pb(II) system

It has been shown in Section 1 that an accumulation of an excess of negative charge by zinc oxide nanoparticles facilitates crossing of a potential barrier of the photoreduction processes. Photocatalytic reduction of lead cations on the surface of ZnO nanoparticles may serve as another perfect example of this phenomenon. On initial stage of the irradiation of colloidal ZnO solutions containing lead acetate, the sole photochemical process is the development of a hypsochromic shift of the edge of ZnO absorption band in the result of the accumulation of excessive electrons by semiconductor nanoparticles (Fig. 6a).

It is known [30] that at radiolytical reduction of Pb(II) one lead atom forms via the disproportionation of two Pb(I) ions. Photocatalytic reduction of Pb(II) to Pb(I) (standard potential of the couple Pb^{2+}/Pb^{+} $E^0 = -1.0$ V versus NHE [30]) by conduction band electrons of 5.0 nm ZnO nanoparticles

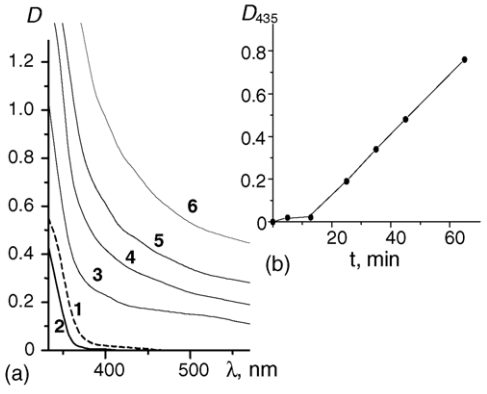

Fig. 6. (a) Absorption spectra of a deaerated colloidal ZnO solution in ethanol in the presence of lead acetate before the irradiation and after 5–65 min exposure. (b) Kinetic curves reflecting accumulation of Pb^0 in the course of the irradiation of deaerated 2-propanolic ZnO colloid containing $Pb(CH_3COO)_2$; $[ZnO] = 2 \times 10^{-3}$ M; $[Pb(CH_3COO)_2] = 5 \times 10^{-4}$ M; light intensity $I = 3.3 \times 10^{-6}$ einstein min^{-1}; $\lambda_{irr} = 310–370$ nm; optical path $l = 1.0$ cm.

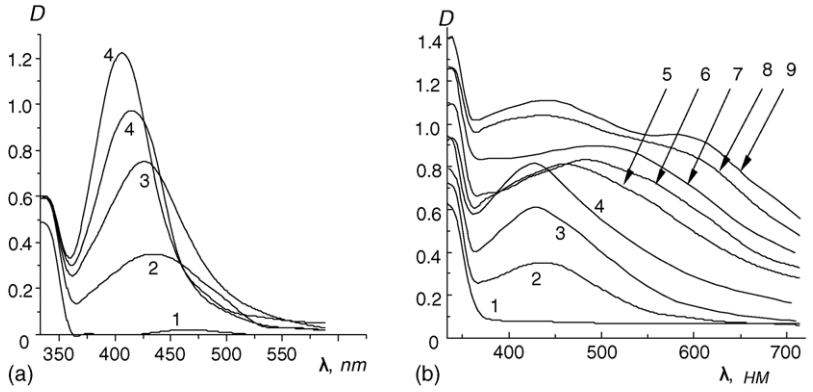

Fig. 7. (a) Absorption spectra of deaerated colloidal ZnO solution containing Ag(I) cations before the irradiation (1) and after the irradiation during 30 s (2), 90 s (3), 120 s (4) and 510 s (5); $[ZnO] = 1 \times 10^{-3}$ M; $[AgNO_3] = 7.5; \times 10^{-5}$ M; light intensity $I = 3.0 \times 10^{-6}$ einstein min^{-1}; cuvette length $l = 1.0$ cm. (b) Absorption spectra of a deaerated colloidal ZnO solution containing $CuCl_2$ and $AgNO_3$ before the irradiation (1) and after the exposure for 1 min (2), 2 min (3), 3 min (4), 9 min (5), 13 min (6), 17 min (7), 52 min (8) and 80 min (9); $[ZnO] = 2 \times 10^{-3}$ M; $[AgNO_3] = 1 \times 10^{-4}$ M; $[CuCl_2] = 5 \times 10^{-4}$ M; light intensity $I = 2.7 \times 10^{-6}$ einstein min^{-1}.

with $E_{CB} = -0.65$ V versus NHE (Table 1) is thermodynamically forbidden. Accumulation of three to four electrons by each ZnO nanoparticles gives them some of the properties of cathodically polarized nanoelectrode. At that, Pb(II) photoreduction becomes possible and proceeds with the constant rate to complete consumption of metal cations (Fig. 6b).

3.4. ZnO–Ag(I)–Cu(II) system

It has been shown in [13] that the irradiation of deaerated ZnO colloids in the presence of Ag(I) results in the formation of silver plasmon bands in the absorption spectra, their maxima shifting gradually to shorter wavelengths in the course of the photoreaction (Fig. 7a). This hypsochromic shift has been associated with an accumulation of excessive electrons by forming ZnO/Ag nanocomposite resulting in an increase in apparent electron density of Ag^0 nanoparticles (N_e) (refer to Equation (VI)).

Irradiation of colloidal ZnO solutions in the presence of Ag(I) and Cu(II) cations results in the evolution of SPR bands differing from that typical for silver and copper nanoparticles in binary ZnO/Ag [13] and ZnO/Cu nanocomposites (compare Fig. 7b with Figs. 7a and 4a). Maxima of silver SPR bands arising in the absorption spectra of ZnO–Ag(I)–Cu(II) systems at initial stages of the illumination are shifted to longer wavelengths, their half-width being noticeably greater in the comparison with undisturbed silver SPR band of binary ZnO/Ag nanocomposites (Table 2). Alterations of the shape and the position of silver SPR bands observed at the co-reduction of Cu(II) with Ag(I) originate apparently from the intercalation of single copper atoms into growing silver nanoparticles and an alteration of the electronic structure of the latters. The maxima of silver plasmon bands in case of simultaneous reduction of Cu(II) and Ag(I) ions are located at longer wavelengths relative to SPR band of pure silver nanoparticles indicating a decrease in electron density in Ag^0 nanoparticles formed in the presence of copper cations. We have therefore concluded that copper atoms intercalated into silver nanoparticles act as electron acceptors [30].

We have studied an effect of the conditions of photocatalytic co-reduction of Cu(II) and Ag(I) induced by ZnO nanoparticles on the parameters of the SPR bands of silver nanoparticles at initial stages of the photoreaction. It has been found that bathochromic shift and broadening of

Table 2
Parameters of plasmon absorption bands of silver nanoparticles forming at co-reduction of Ag^+ and Cu^{2+} ions on the surface of ZnO nanoparticles

$[Ag^+] \times 10^4$ (M)	$[Cu^{2+}] \times 10^4$ (M)	Deaeration	λ_{max} (nm)	w_{max} (nm)
2.0	–	–	428	94
2.0	0.25	–	430	119
2.0	0.50	–	453	145
2.0	1.00	–	463	151
0.5	2.0	+	453	129
1.0	2.0	+	440	110
2.0	2.0	+	440	110
1.0	–	+	428	81
1.0	0.2	+	432	97
1.0	0.5	+	437	100
1.0	1.0	+	440	105
1.0	2.0	+	446	108
1.0	5.0	+	447	121

silver plasmon bands in the comparison with undisturbed Ag^0 plasmon bands become more pronounced at an increase in the $[Cu^{2+}]/[Ag^+]$ ratio (Table 2), and at constant $[Cu^{2+}]/[Ag^+]$—with an increase in the exposure time. It has been mentioned above that the photoreduction of Cu(II) on the surface of ZnO nanoparticles is slow, the rate-limiting stage being the discharge of Cu(II) cations by ZnO conduction band electrons. The photoreduction of silver ions is faster reaction. It results in the formation of catalytic centers $(Ag^0)_x$ facilitating Cu(II) reduction and increasing the quantity of intercalated copper and consequent deformation of silver SPR absorption band. Accumulation of Ag^0 on the surface of ZnO nanoparticles leads to a decrease of Ag(I) concentration and to a growth of the probability of Cu(II) photoreduction. The influence of Cu^0 on optical properties of silver nanoparticles (Fig. 7, curves 5–7) indicates that copper deposition does take place on the surface of silver component of ZnO/Ag nanocomposite. Further increase in the quantity of deposited Cu^0 results in the apparition of characteristic optical features of Cu^0 nanoparticles with formed individual electronic structure—plasmon resonance band centered at 620 nm (Fig. 7, curves 8 and 9). So, the irradiation of colloidal ZnO solutions containing Ag(I) and Cu(II) cations results in the formation of ternary bimetallic nanocomposites where the metal component of the composite, i.e. bimetallic Ag/Cu nanoparticles have apparently "core–shell" structure [38–40]. Similar evolution of absorption spectra in the course of bimetallic "core–shell" nanoparticles formation has been also observed in other systems such as Ag/Au [6,30,41–46], Ag/Pt, Au/Pt [14], Au/Pd [14,47].

Contact of ZnO/Ag/Cu nanoparticles with oxygen results in the reverse transformation of the absorption spectra due to the oxidation of Cu^0. Copper SPR band at $\lambda = 620$ nm gradually disappears, while the maximum of silver SPR band shifts to shorter wavelengths.

3.5. ZnO–Ag(I)–Cd(II) and ZnO–Ag(I)–Zn(II) systems

It has been found that optical properties of ethanolic solutions containing ZnO nanoparticles with $2R = 6.0$ nm and Cd(II) cations remain unchanged at prolonged irradiation. This fact indicates that the ZnO conduction band electrons do not reduce Cd(II) ions. In case of smaller ZnO nanoparticles, anodic photocorrosion of the semiconductor is observed (refer to Section 1).

The illumination of colloidal ZnO solutions in the presence of a mixture of Ag(I) and Cd(II) cations results in the evolution of silver plasmon bands centered at 420–425 nm (Fig. 8a). At further exposure, both growth rate of silver SPR bands and hypsochromic shift of plasmon maxima gradually slow down. However, in contrast to ZnO–Ag(I) systems, a hypsochromic shift of Ag^0 SPR band is much more prononced in ZnO–Ag(I)–Cd(II) system (Fig. 8b). Analysis of the expression (V) shows that this effect may be associated with an accumulation of greater negative charge on ZnO/Ag nanoparticles forming at the illumination of colloidal solutions containing both Ag(I) and Cd(II) cations in the comparison with binary ZnO–Ag(I) system. Similar phenomenon has been observed in [48–50] at radiolytic deposition of metallic cadmium on the surface of silver nanoparticles. This effect has been associated with partial transfer of electron density from Cd^0 atoms to Ag^0 nanoparticles. Electron density transfer from Cd^0 to Ag^0 is driven by a difference in Fermi levels of the metals and stops after the equilibration of these energies [30,48–50]. So, we have concluded that the irradiation of ZnO–Ag(I)–Cd(II) system after the formation of silver nanoparticles and consumption of the greater part of Ag(I) cations induces Cd^0 photodeposition on the surface of silver nanoparticles and subsequent formation of ternary bumetallic ZnO/Ag/Cd nanocomposites.

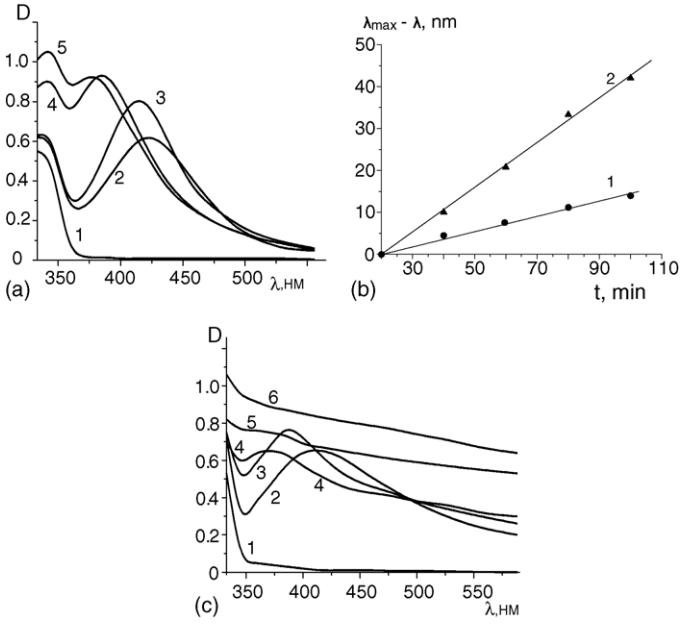

Fig. 8. (a) Absorption spectra of a deaerated colloidal ZnO solution containing $AgNO_3$ and $Cd(CH_3COO)_2$ before the irradiation (1) and after the exposure for 5 min (2), 10 min (3), 20 min (4) and 30 min (5); $[ZnO] = 1 \times 10^{-3}$ M; $[AgNO_3] = 1 \times 10^{-4}$ M; $[Cd(CH_3COO)_2] = 1 \times 10^{-4}$ M. (b) A change of the position of the maximum of silver plasmon absorption band at the irradiarion of colloidal ZnO solution in the presence of Ag(I) ions (1) or a mixture of Ag(I) and Cd(II) (2). (c) Absorption spectra of deaerated ethanolic ZnO colloid containing $AgNO_3$ before the irradiation (1) and after the exposure for 0.3 min (2), 1 min (3), 20 min (4), 55 min (5) and 80 min (6); $[ZnO] = 2 \times 10^{-3}$ M; $[AgNO_3] = 1 \times 10^{-4}$ M; light intensity $I = 2.7 \times 10^{-6}$ einstein min^{-1}.

The irradiation of ethanolic ZnO sols with $2R < 6.0$ nm (able to undergo cathodic photocorrosion with the formation of ZnO/Zn nanocomposites) in the presence of $AgNO_3$ results at small exposures in the formation of composite ZnO/Ag nanoparticles (Fig. 8c, curves 1–3). The maximum of silver plasmon band in this case is also shifted more pronouncedly to shorter wavelengths than at the irradiation of colloidal ZnO nanoparticles of greater size, which are not able to photocorrode. Such modification of absorption spectra of ZnO/Ag nanocomposite is associated, in our opinion, with the formation of Zn^0 metal, able, like Cd^0, to transfer the electron

density to silver nanoparticles changing in that way their optical properties. Prolonged irradiation of solutions results in the rise of an absorption band characteristic for Zn^0 (Fig. 8c, curves 4–6), while silver SPR band is entirely masked by deposited zinc. So, the combination of two reactions – the photocorrosion of ZnO nanoparticles and Ag(I) photoreduction – gives ternary ZnO/Ag/Zn nanocomposites.

4. Conclusions

We have discussed the synthesis of colloidal zinc oxide nanoparticles of different size in ethyl alcohol, their optical properties and energetic characteristics. It has been found that the stationary irradiation of ZnO sols results in a hypsochromic shift of the long-wave edge of their absorption bands due to dynamic Burstein–Moss effect. This shift is followed by photocorrosion of semiconductor nanoparticles, the rate of the photoreaction increasing at a decrease of their average diameter. The examination of energetic characteristics of ZnO nanoparticles of different sizes has shown that an increase of the rate of the photocorrosion is associated with quantum confinement effects in ZnO nanocrystals, i.e. growth of the reduction potential of ZnO conduction band beyond Fermi level of cathodic photodecomposition of semiconductor nanoparticles.

Peculiarities of the photocatalytic reduction of copper ions as well as co-reduction of Cu(II) with Ag(I) on the surface of ZnO nanocrystals have been studied. It has been shown that the former reaction results in the formation of binary ZnO/Cu nanocomposite whereas in the latter case the photoreaction gives ternary bimetallic ZnO/Ag/Cu structures, their composition and optical properties depending on the synthesis conditions and the composition of reaction mixture.

It has been established that ZnO nanoparticles can catalyze the photoreduction Pb(II) ions. The effect of excessive negative charge accumulated at the irradiation by ZnO nanoparticles on their ability to participate in this reaction has been discussed.

The processes of ternary bimetallic ZnO/Ag/Cd and ZnO/Ag/Zn nanocomposites formation have been investigated. It has been found that cadmium or zinc metals deposition onto the surface of silver nanoparticles forming in the course of photocatalytic Ag(I) reduction over ZnO nanoparticles results in a hypsochromic shift of the maximum of silver plasmon absorption band. This shift has been associated with partial transfer of the electron density from Cd^0 or Zn^0 to Ag^0 nanoparticles.

References

[1] A. Wood, M. Giersig, P. Mulvaney, J. Phys. Chem. B 105 (2001) 8810.
[2] A.I. Kulak, Electrochemistry of Semiconductor Heterostructures, Universitetskoye, Minsk, 1986.
[3] R.F. Khairutdinov, Russ. Chem. Rev. 67 (1998) 125.
[4] L.C. Chen, F.-R. Tsai, C.-M. Huang, J. Photochem. Photobiol. A Chem. 170 (2004) 7.
[5] J.-K. Yang, S.-K. Lee, J. Colloid Interface Sci. 282 (2005) 5.
[6] E. Szabó-Bárdos, H. Czili, A. Horváth, J. Photochem. Photobiol. A Chem. 154 (2003) 195.
[7] H.M. Sung-Suh, J.R. Choi, H.J. Hah, S.M. Koo, Y.C. Bae, J. Photochem. Photobiol. A Chem. 163 (2004) 37.
[8] C. He, Y. Xiong, J. Chen, C. Zha, X. Zhu, J. Photochem. Photobiol. A Chem. 157 (2003) 71.
[9] S. Yamazaki, N. Takemura, Y. Yoshinaga, A. Yoshida, J. Photochem. Photobiol. A Chem. 161 (2003) 57.
[10] A. Yamakata, T. Ishibashi, H. Onishi, J. Photochem. Photobiol. A Chem. 160 (2003) 33.
[11] V. Vamathevan, R. Amal, D. Beydoun, G. Low, S. McEvoy, J. Photochem. Photobiol. A Chem. 148 (2002) 233.
[12] T. Lee, J. Liu, N.-P. Chen, R.P. Andres, D.B. Janes, R. Reifenberg, J. Nanopart. Res. 2 (2000) 345.
[13] A.L. Stroyuk, V.V. Shvalagin, S.Ya. Kuchmii, Theor. Exp. Chem. 40 (2004) 94.
[14] N. Toshima, T. Yonezawa, New J. Chem. (1998) 1179.
[15] A.V. Vorontsov, V.P. Dubovitskaya, J. Catal. 221 (2004) 102.
[16] N.-L. Wu, M.-S. Lee, Int. J. Hydrogen Energy 29 (2004) 1601.
[17] H. Selcuk, W. Zaltner, J.J. Sene, M. Bekbolet, M.A. Anderson, J. Appl. Electrochem. 34 (2004) 653.
[18] A.P. Shpak, Y.A. Kunitski, O.O. Korotchenkov, S.Y. Smyk, Quantum Low-dimension Systems, Akademperiodika, Kyiv, 2003.
[19] V.M. Arutyunyan, Semiconductor photoelectrodes for photoelectrochemical conversion of solar energy, in: K.I. Zamaraev (Ed.), Photocatalytic Conversion of Solar Energy, vol. 1, Nauka, Novosibirsk, 1985.
[20] D.W. Bahnemann, C. Kormann, M.R. Hoffmann, J. Phys. Chem. 91 (1987) 3789.
[21] D.W. Bahnemann, Isr. J. Chem. 33 (1993) 115–136.
[22] A. van Dijken, E.A. Meulenkamp, D. Vanmaekelbergh, A. Meijerink, J. Phys. Chem. B 104 (2000) 4355.
[23] N.S. Pesika, K.J. Stebe, P.C. Searson, J. Phys. Chem. B 107 (2003) 10412.
[24] E.M. Wong, P.G. Hoertz, C.J. Liang, B.-M. Shi, G.J. Meyer, P.C. Searson, Langmuir 17 (2001) 8362.
[25] P. Hoyer, H. Weller, J. Phys. Chem. 99 (1995) 14096.
[26] G.H. Schoenmakers, D. Vanmaekelbergh, J.J. Kelly, J. Chem. Soc. Faraday Trans. 96 (1997) 1127.
[27] A.I. Kryukov, S.Ya. Kuchmii, V.D. Pokhodenko, Theor. Exp. Chem. 36 (2000) 69.
[28] C. Liu, A.J. Bard, J. Phys. Chem. 93 (1989) 3231.
[29] L.I. Antropov, Theoretical Electrochemistry, Vysshaya shkola, Moscow, 1965.
[30] A. Henglein, J. Phys. Chem. 97 (1993) 5457.
[31] A. Henglein, J. Phys. Chem. B 104 (2000) 1206.
[32] J.P. Cason, M.E. Miller, J.B. Thompson, C.B. Roberts, J. Phys. Chem. B 105 (2001) 2297.
[33] A.V. Loginov, V.V. Gorbunova, T.B. Boitsova, J. Nanopart. Res. 4 (2002) 193.
[34] A.C. Curtis, D.G. Duff, P.P. Edwards, D.A. Jefferson, F.G. Johnson, A.I. Kirkland, A.S. Wallace, J. Phys. Chem. 92 (1988) 2270.
[35] I. Lisiecki, M.P. Pileni, J. Phys. Chem. 99 (1995) 5077.
[36] M.P. Pileni, New J. Chem. (1998) 693.
[37] Y.Y. Fialkov, V.F. Grishtchenko, Metals Electrodeposition from Nonaqueous Solutions, Naukova dumka, Kyiv, 1985.
[38] T.B. Boitsova, V.V. Gorbunova, A.V. Loginov, N.N. Ivanova, Russ. J. Phys. Chem. 73 (1999) 1127.
[39] A.V. Toporko, V.V. Tsvetkov, V.D. Yagodovski, Russ. J. Phys. Chem. 70 (1996) 1794.
[40] A.V. Toporko, V.V. Tsvetkov, V.D. Yagodovski, A. Issa, Russ. J. Phys. Chem. 71 (1997) 1095.

[41] J.H. Hodak, A. Henglein, M. Giersig, G.V. Hartland, J. Phys. Chem. B 104 (2000) 11708.
[42] E. Hutter, J.H. Fendler, Chem. Commun. (2002) 378.
[43] D.-H. Chen, C.-J. Chen, J. Mater. Chem. 12 (2002) 1557.
[44] C. de Cointet, J. Khatouri, M. Mostafavi, J. Belloni, J. Phys. Chem. B 101 (1997) 3517.
[45] I. Lee, S.W. Han, K. Kim, Chem. Commun. (2001) 1782.
[46] C.S. Ah, S.D. Hong, D.-J. Jang, J. Phys. Chem. B 105 (2001) 7871.
[47] Y. Mizukoshi, K. Okitsu, Y. Maeda, T.A. Yamamoto, R. Oshima, Y. Nagata, J. Phys. Chem. B 101 (1997) 7033.
[48] A. Henglein, J. Lilie, J. Phys. Chem. 85 (1981) 1246.
[49] A. Henglein, M. Gutierez, E. Janata, B.G. Ershov, J. Phys. Chem. 96 (1992) 4597.
[50] A. Henglein, P. Mulvaney, T. Linnert, A. Holzwarth, J. Phys. Chem. 96 (1992) 2411.